

Moisture Property and Thermal Behavior of Two Novel Synthesized Polyol Pyrrole Esters in Tobacco

Wenpeng Fan, Haiying Tian,[§] Hongli Chen,[§] Wenjuan Chu, Lu Han, Pengyu Li, Ziting Gao, Xiaoming Ji,^{*} and Miao Lai^{*}



Cite This: *ACS Omega* 2023, 8, 4716–4726



Read Online

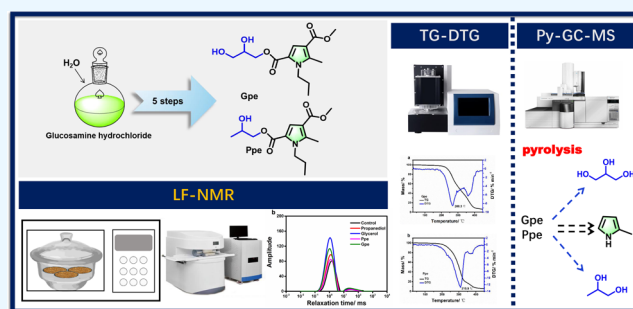
ACCESS |

Metrics & More

Article Recommendations

Supporting Information

ABSTRACT: To overcome the shortcomings of high relative humidity and harmful oxidation products from traditional humectants, excellent humectants and flavor precursors were reported herein. Glucosamine hydrochloride was used as the starting material for the cyclization, oxidation, and alkylation processes that produced pyrrole acid. Then, esterification occurred with polyol catalyzed by EDC and DMAP to give the target compounds 2-(2,3-dihydroxypropyl) 4-methyl 5-methyl-1-propyl-1H-pyrrole-2,4-dicarboxylate (Gpe) and (2-hydroxypropyl) 4-methyl 5-methyl-1-propyl-1H-pyrrole-2,4-dicarboxylate (Ppe). Nuclear magnetic resonance (¹H NMR, ¹³C NMR), infrared spectroscopy (IR), and high-resolution mass recorded spectrometry (HRMS) were used to confirm the two novel polyol pyrrole ester compounds. When Gpe and Ppe were added to the tobacco shred, low-field nuclear magnetic resonance (LF-NMR) imaging was applied to assess the hygroscopicity and moisturizing capacity. Furthermore, thermogravimetry (TG) and pyrolysis–gas chromatography/mass spectrometry (Py-GC/MS) techniques were applied to study their thermal behaviors. These results showed that the target compounds (Gpe and Ppe) are good humectants with thermal properties of high-temperature stability and flavor release.



1. INTRODUCTION

The economic importance of tobacco makes it one of the most often researched plants, which is an extremely important industrial production in China.^{1,2} The quality of the final tobacco products in the industry not only depends on simply the tobacco shred's moisture level but also is a matter of smoking characteristics of dry flue gas, pungent, insufficient flavor, etc.^{3,4} It has always been a bottleneck technology of moisture retentivity and flavor enhancement to improve the quality of cigarettes in China. As a result of their polyhydroxy structure, polysaccharides can adsorb water and form a membrane on the surface of tobacco to reduce the loss of water, which featured excellent moisture adsorption and retention used in clinical medicine, cosmetics, and food preservation.^{5–7} For example, the novel polysaccharide derived from *Phyllobacterium* sp. 921F exhibited favorable rheological properties and excellent moisture retention ability.⁸ However, some polysaccharides are generally limited to compare their humectant properties with those of synthetic glycerin for their physicochemical properties, including poor water solubility, low molecular weight, and branching degree. In addition, glycerol, propylene glycol, and sorbitol are examples of polyol compounds (traditional humectants) that have been widely employed in tobacco production for moisture adsorption and retention.^{9,10} These compounds show excellent moisture

retention activities, mainly because water molecules might form hydrogen bonds with their hydroxyl groups.¹¹ However, this property of traditional humectants could accelerate the deterioration of the tobacco quality, resulting from the increase of the amount of moisture in the tobacco crumble, which held in high relative humidity (RH) for long. Additionally, smoking tobacco may produce hazardous substances such as propylene oxide, acrolein, etc.¹² Therefore, to assure the quality of the final tobacco products, a modified and innovative humectant with moisture absorption and desorption and cigarette flavor improvement deserves to be developed.

On the other hand, pyrrole derivatives are generated from bread, nut, coffee, cigarettes, and other toasted food, which are highly valuable compounds in perfume and possess characteristic aroma or organoleptic properties such as bitterness, roasted, peanutty, buttery, and meaty, usually used as food flavor additives.^{13–17} Recently, the cigarette and food fields have paid pyrrole derivatives a lot of attention due to their

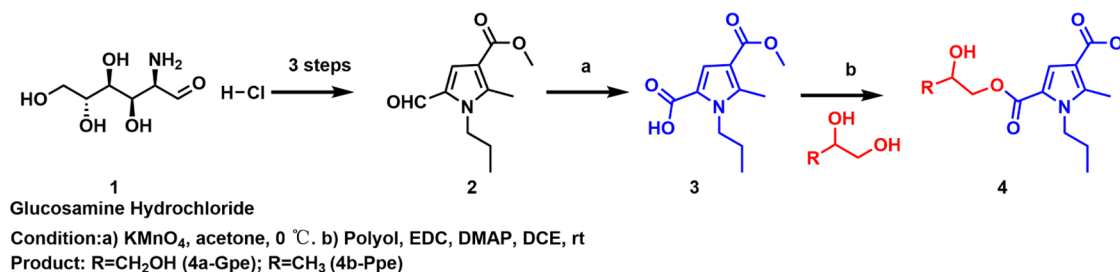
Received: October 17, 2022

Accepted: January 17, 2023

Published: January 27, 2023



Scheme 1. Synthesis Route of Gpe and Ppe



exceptional flavoring abilities.^{18,19} Under the conditions of the cigarette smoking process, the pyrolysis products of heterocyclic derivatives, which contain a variety of tobacco fragrance ingredients, including pyrrole, 2,5-dimethylpyrrole, 2-acetylpyrrole, etc., can enhance the flavor of cigarettes.²⁰ The structural motifs of polyol derivatives could be designed by esterification from glycerol and pyrroles, which are expected to be used in cigarette moisturizing and flavoring enhancement techniques because of the properties of hydrophilicity, thermal stability, and being precursors of aroma substances. Consequently, it is crucial to study and make use of the qualities of polyol pyrrole esters in cigarette moisturizing and flavor enhancement during the smoking process. To evaluate the hygroscopicity and moisturizing properties, nuclear magnetic resonance (NMR) could be used for nondestructive characterization of the quality and water distribution and migration in various fruit,^{21–24} plant,^{25,26} and vegetable^{27–29} tissues. Moreover, the high-temperature stability and decomposition mechanism of polyol pyrrole esters on the tobacco shred during cigarette burning were evaluated using TG and Py-GC/MS.^{30–32}

In this study, the two target compounds 2-(2,3-dihydroxypropyl) 4-methyl 5-methyl-1-propyl-1H-pyrrole-2,4-dicarboxylate (Gpe) and (2-hydroxypropyl) 4-methyl 5-methyl-1-propyl-1H-pyrrole-2,4-dicarboxylate (Ppe) were first synthesized *via* the reactions of cyclization, oxidation, alkylation, and esterification using glucosamine hydrochloride as the starting ingredient. Then, the hygroscopicity and moisturizing properties of the glycerol pyrrole esters used on the tobacco shred were evaluated. The dynamic models related to moisture adsorption and desorption of tobacco shred samples have been established. Transverse relaxation time (T_2), which was established using LF-NMR, was used to measure the moisture conditions and ratio in the tobacco shred. In addition, investigation of the polyol pyrrole esters's pyrolysis products and thermal stability was done using TG-DSC and Py-GC/MS methods. The results of the moisture properties and thermal behavior of polyol pyrrole esters are expected to provide a theoretical basis and key technology for the use of polyol pyrrole esters in tobacco shred moisturizing and flavor enhancement support. It is of great significance to further enhance the market competitiveness of Chinese cigarettes by improving the moisture retention of tobacco and narrowing the gap with well-known foreign brands.

2. MATERIALS AND METHODS

2.1. Preparation of the Target Compounds and Structure Identification. All the chemicals and solvents used in this investigation were commercial grade and were bought from Tianjin Kermel Chemical Reagent Co., Ltd. (China). Furthermore, NMR, IR, and HRMS measurements

supported the structures of novel target compounds, such as a BRUKER/AVANCE NEO 400 MHz (BioSpin GmbH, dissolvent of CDCl_3 with tetramethylsilane TMS), Fourier transform infrared spectrophotometer (Nicolet iS50, Thermo Nicolet Co, Waltham, MA), and Waters Micromass Q-TOF (Micro TM, Agilent).

2.1.1. Synthesis of 2-Pyrrolecarboxylic Acid Derivative (3). Glucosamine was used as the starting material for the synthesis of compound 2, which involved cyclization, oxidation, and alkylation in 80% yield.¹⁹ As shown in Scheme S.1, in a round-bottom flask with a magnetron, compound 2, KMnO_4 (2.0 equiv), and acetone/ H_2O ($v:v = 1:1$) were added and stirred for 2 h at $0\text{ }^\circ\text{C}$. TLC (petroleum ether/ethyl acetate: 2/1) was used to confirm that the reaction was complete. Acetone was then extracted using a vacuum, and its aqueous solution was acidified with aq HCl (4 M) to a pH of 2; then, 3 mL of aq NaHSO_3 (10%) was added. Ethyl acetate was used to extract the combination, and the mixed organic extracts were then washed with brine and water, dried over MgSO_4 , and concentrated. By recrystallization, the anticipated compound 3 was obtained with 65% yield (516 mg).

2.1.2. Synthesis of Polyol Pyrrole Esters (Gpe and Ppe). EDC (1.0 mmol) and compound 3 (1.2 mmol) in an anhydrous DCM (10 mL) mixture were stirred at room temperature in 2 h. DMAP (0.02 mmol) and glycerol or 1,2-propanediol (1.0 mmol) were then added, and the mixture was agitated for 10 h. TLC was used to monitor the reaction's completion. After the mixture had been evaporated, ethyl acetate and water were added, successively. The organic phase was separated and dried overnight with anhydrous Na_2SO_4 . Following column chromatography on a silica gel (100 mesh) and elution in a 20:1 petroleum ether/ethyl acetate solution, the crude residue was refined to provide Gpe (compound 4a, 233 mg, 65% yield) and Ppe (compound 4b, 204 mg, 60% yield). The reaction route is shown in Scheme 1.

2.2. Hygroscopicity and Moisturizing. **2.2.1. Preparation of the Experimental Samples.** First, the prepared tobacco shred was acclimated for 72 h at $22\text{ }^\circ\text{C}$ and 60% RH. Then, glycerol, 1,2-propanediol, Ppe, and Gpe were equally sprayed on the surface of the tobacco shred, which increased the solute content to 2.0% (wt) weight of tobacco (5 g), and the tobacco shred sprayed with the same quality of distilled water was set as the control group (Figure 1). The processed tobacco shred was acclimated for 72 h at $22\text{ }^\circ\text{C}$ and 60% RH. Subsequently, the tobacco shred was mixed with saturated magnesium chloride solution (200 mL) and put in desiccators (32% RH, $22\text{ }^\circ\text{C}$) and saturated potassium chloride solution (200 mL) for (84% RH, $22\text{ }^\circ\text{C}$). The weighing technique was used to estimate the sample's initial moisture content, and the reduction in moisture during storage was used to calculate the sample's change in the moisture content.³³



Figure 1. Tobacco shred added with different polyol materials.

2.2.2. Model Evaluation Methods. The dry basis moisture content of the tobacco shred was converted into the moisture ratio (MR) according to Formula 1, which accurately reflected the moisture content of the cut tobacco on a dry basis at different times

$$\text{MR} = \frac{M_t - M_e}{M_0 - M_e} \quad (1)$$

where M_e is the dry basis moisture content (%), M_t is the dry basis moisture content at t (h) (%), and M_0 is the initial dry basis moisture content (%).

2.2.3. Establishment of the Dynamic Model. Many models related to adsorption and desorption have been proposed, such as Brunauer–Emmett–Teller (BET) model and Guggenheim Anderson-de Boer (GAB) model.⁴⁰ In this study, we tested these models, in which the values of RMSE were too large to accurately reflect the process of water adsorption on the cut tobacco. Among them, the more trustworthy were logistic model, Poly4 model, and cubic model, which were used to describe the change process of adsorption kinetics and analytical kinetics. The experimental data were adapted for the Origin program using a nonlinear fitting (version 19.0, OriginLab Inc., Northampton, MA).

$$\text{logistic: } \text{MR} = b + \frac{(a - b)}{\left(1 + \left(\frac{t}{c}\right)^d\right)} \quad (2)$$

$$\text{Poly4: } \text{MR} = a + bt + ct^2 + dt^3 + et^4 \quad (3)$$

$$\text{cubic: } \text{MR} = a + bt + ct^2 + dt^3 \quad (4)$$

where the constants for the three models are a , b , c , d , and e . The correlation coefficient (R^2) and the root-mean-square

error (RMSE) can be used to assess the model fitting results. The model that gives the minimum value of RMSE and the maximum value of R^2 is the most reliable. R^2 and RMSE were calculated according to Formulas 5 and 6, respectively

$$R^2 = \sum_i^N \frac{(\text{MR}_{\text{pre},i} - \overline{\text{MR}_{\text{pre},i}})^2}{(\text{MR}_{\text{exp},i} - \overline{\text{MR}_{\text{exp},i}})^2} \quad (5)$$

$$\text{RMSE} = \left[\frac{1}{N} \sum_i^N (\text{MR}_{\text{pre},i} - \text{MR}_{\text{exp},i})^2 \right]^{1/2} \quad (6)$$

where N is the number of experimental observations, MR_{exp} is the moisture content experimental value, and MR_{pre} is the moisture content predicted by the model.

2.2.4. LF-NMR Analysis. The moisture state and ratio in the tobacco shred were assessed by measuring the transverse relaxation time (T_2) determined using a PQ001 MicroMR Cabinet NMR imager (Shanghai Niumai Electronic Technology Co., Ltd.). The preparation of tobacco samples was consistent with Section 2.2.1. To attain constant weights, all samples were equilibrated at 22 °C with RH values of 32 and 84%. A total of 1.5 g of each group was weighed and put into the NMR sample tube (1 cm × 3.5 cm) for analysis, and three parallel experiments were set up. The CPMG pulse sequence was used to undertake data capture once the FID sequence had calibrated the resonant center frequency. The following are the CPMG sequence's parameters: probe coil diameter: 18 mm; magnet temperature: 32.00 ± 0.01 °C; resonance frequency (SF) = 22 MHz; offset frequency (O1) = 778 183.37 Hz; pulse time (P1) = 21 μs; number of data points (TD) = 239 994; repeated sampling waiting time (TW) = 5000.000 ms; pulse time (P2) = 40 μs; echo time (TE) = 0.300 ms; NECH = 8000; spectral width (SW) = 100 KHz; radio frequency delay (RFD) = 0.080 ms; analog gain (RG1) = 3 db; DR = 3; and NS = 32 echo time. Inversion of the T_2 decay curve finally led to the observation of transverse relaxation time (T_2) spectra.

2.2.5. Statistical Analysis. Three separate experiments were conducted under the same conditions. Nonlinear fitting was conducted using Origin 2019b. R_2 and RMSE were used to evaluate the accuracy of the regression equations. Results were presented as mean values using IBM's SPSS version 19.0 (Armonk, New York), and significance was defined as $P < 0.05$.

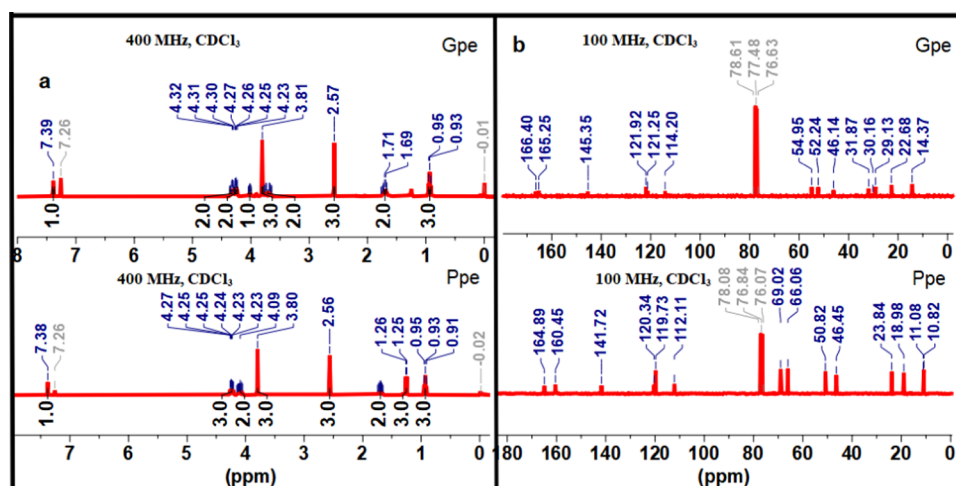


Figure 2. ^1H NMR (a) and ^{13}C NMR (b) of Gpe and Ppe.

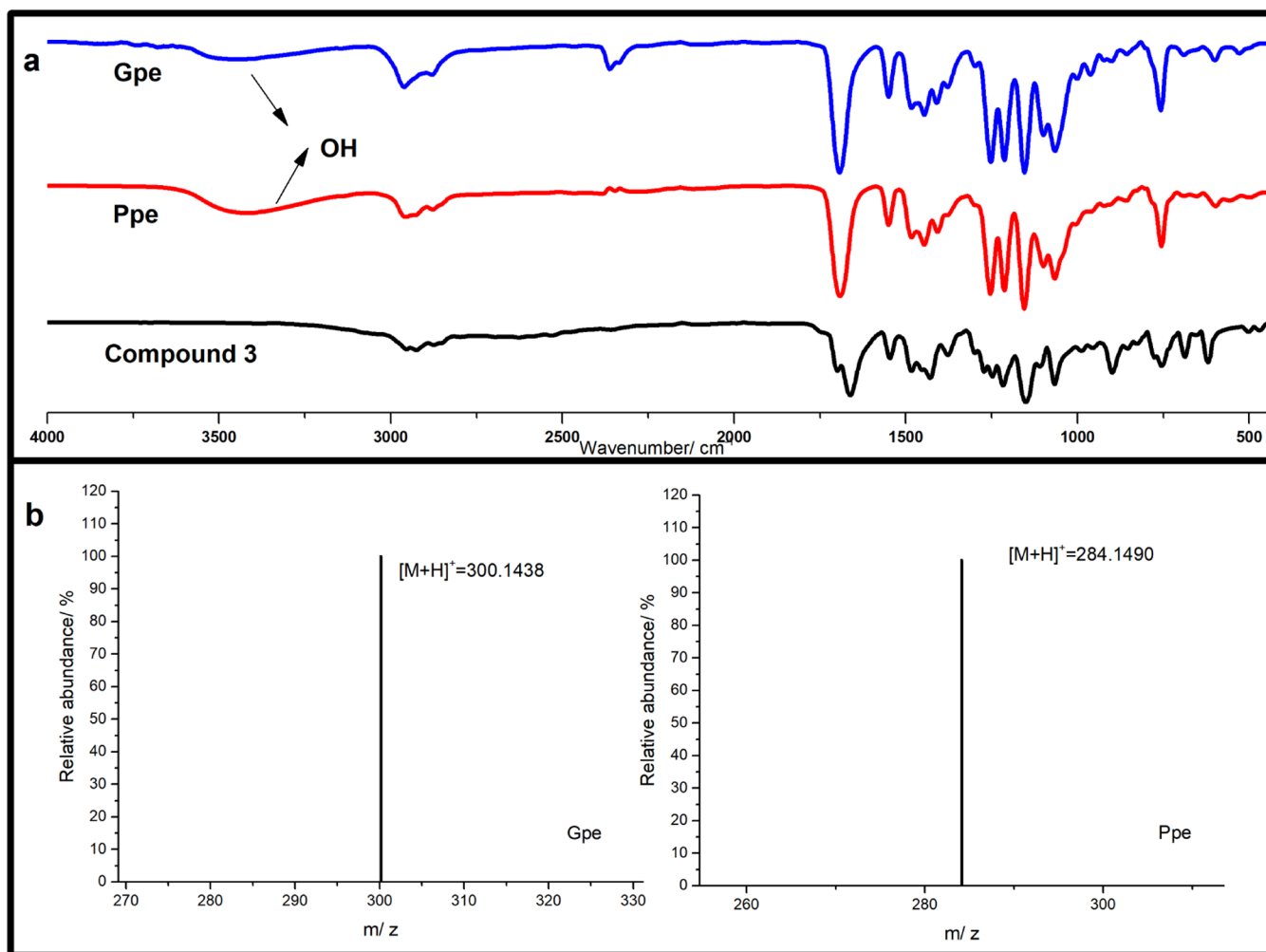


Figure 3. FTIR (a) and HRMS (b) of Gpe and Ppe.

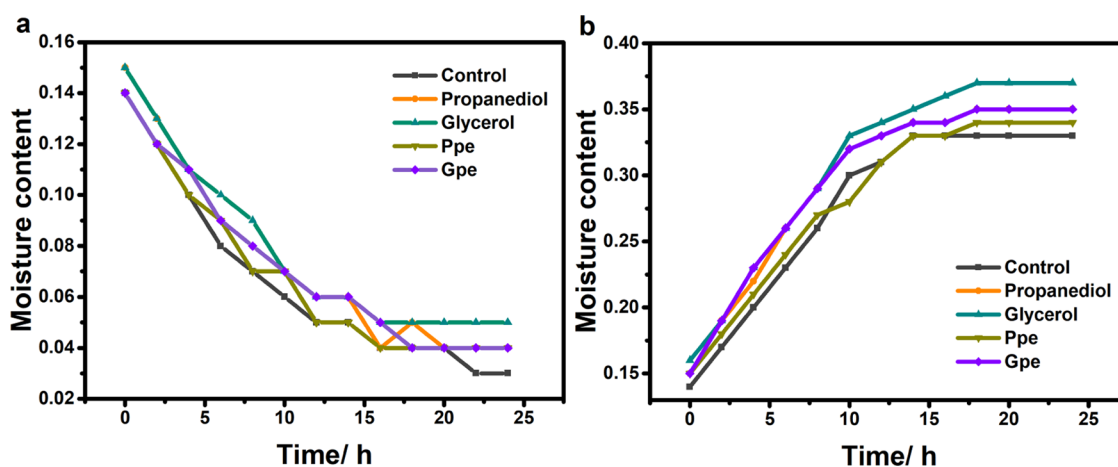


Figure 4. Moisture contents of the tobacco shred at 22 °C and RH = 32% (a) and RH = 84% (b).

2.3. Thermal Behavior Analysis. **2.3.1. TG Analysis.** A simultaneous thermal analyzer gave the TG-DTG and DSC curves of Gpe and Ppe (STA 449 F3, Netzsch, Germany). Each time, a sample of 3 mg was maintained, and spectrally pure Al₂O₃ served as a reference. Each experiment used an air environment with a flow rate of 60 mL min⁻¹ and was heated at a rate of 10 °C min⁻¹ between 30 and 450 °C.

2.3.2. Pyrolysis Analysis. Py-GC/MS analysis was applied to identify the pyrolysis products of Gpe and Ppe (Pyroprobe 5250T, CDS, Analytical Inc., and Agilent 7890/5975). About 2 mg of each sample was placed in a 25 mm quartz tube to fracture for 10 s at the predetermined temperatures. 350 and 400 °C were set aside as the pyrolysis temperatures. The reactor was first heated at the rate of 6 °C min⁻¹ and

Table 1. Estimated Values for the Fitting Models (RH = 32%, 22 °C)

group	logistic		Poly4		cubic	
	R ²	RMSE	R ²	RMSE	R ²	RMSE
control	0.9655	0.6674	0.9999	0.0001	0.9986	0.1239
glycerol	0.9518	0.6791	0.9999	0.0001	0.9986	0.1363
propanediol	0.9612	0.6541	0.9999	0.0001	0.9986	0.1363
Ppe	0.9812	0.6741	0.9999	0.0001	0.9986	0.1265
Gpe	0.9732	0.9138	0.9999	0.0001	0.9986	0.1283

Table 2. Estimated Values for the Fitting Models (RH = 84%, 22 °C)

group	logistic		Poly4		cubic	
	R ²	RMSE	R ²	RMSE	R ²	RMSE
control	0.8563	0.8143	0.9999	0.0001	0.9365	0.0210
glycerol	0.9608	1.7190	0.9999	0.0001	0.9526	0.0146
propanediol	0.9612	0.6441	0.9999	0.0001	0.9436	0.1263
Ppe	0.9812	0.5641	0.9999	0.0001	0.9682	0.1435
Gpe	0.9149	0.9329	0.9999	0.0001	0.9252	0.0163

maintained at 50 °C. The trials were conducted in an air environment.

A capillary column DB-5MS (30 m × 250 μm × 0.25 μm) was used for the chromatographic separation. The intended injection port temperature was 300 °C. The oven's initial temperature was set at 50 °C; then, it was increased to 80 °C at a rate of 6 °C min⁻¹ and then to 110 °C and kept there for 2 min. After 2 min, the oven had reached a final temperature of 280 °C at a rate of 5 °C min⁻¹. With no splits, helium was used as the carrier gas at a flow rate of 1 mL min⁻¹.

A mass spectrometer was used to examine the separated components. The transfer line was heated to 300 °C, and the energy of EI was fixed at 70 eV. The quadrupole temperature was 150 °C, while the ion source temperature was specified at 230 °C. From 30 to 500 *m/z*, mass spectra were collected, and the solvent delay time was 2.8 min. The mass spectrum library (NIST17) that was connected to the GC/MS apparatus was used to match the pyrolysis products.

3. RESULTS AND DISCUSSION

3.1. Characterization of the Target Compounds Gpe and Ppe.

The structures of Gpe and Ppe were characterized

Table 3. Fitting Results of Poly4 Models (RH = 32%, 22 °C)

group	<i>a</i>	<i>b</i>	<i>c</i>	<i>d</i>	<i>e</i>
control	0.4097	0.9354	0.0179	0.0003	0.0001
glycerol	0.4622	0.8354	0.0040	0.0010	0.0002
propanediol	0.4325	0.8553	0.0032	0.0011	0.0005
Ppe	0.4322	0.8354	0.0032	0.0013	0.0003
Gpe	0.3465	0.9237	0.0283	0.0006	0.0004

Table 4. Fitting Results of Poly4 Models (RH = 84%, 22 °C)

group	<i>a</i>	<i>b</i>	<i>c</i>	<i>d</i>	<i>e</i>
control	1.2751	0.4545	0.1877	0.0140	0.0003
glycerol	0.2648	1.7797	0.0210	0.0015	0.0001
propanediol	0.2528	1.2737	0.0112	0.0023	0.0002
Ppe	0.6438	1.4736	0.0372	0.0043	0.0002
Gpe	0.6193	1.9962	0.0352	0.0022	0.0001

by ¹H and ¹³C NMR, as shown in (Figure 2a,b). The major signals of the H atom in the pyrrole appeared at 7.39 ppm, and

the corresponding signals of non-heterocyclic H occurred at 4.37–0.94 and 4.25–0.94 ppm, respectively. The major signals of the C atom in pyrrole and O–C=O were in the low-field area, while the others moved to the high-field region. The H and C atom signals were as follows.

2-(2,3-Dihydroxypropyl) 4-methyl 5-methyl-1-propyl-1H-pyrrole-2,4-dicarboxylate (Gpe): ¹H NMR (400 MHz, Chloroform-*d*) δ 7.39 (s, 1H), 4.37–4.30 (m, 2H), 4.28–4.24 (m, 2H), 4.03 (q, *J* = 5.1 Hz, 1H), 3.81 (s, 3H), 3.77–3.65 (m, 2H), 2.58 (s, 3H), 1.70 (d, *J* = 7.7 Hz, 2H), 0.94 (t, *J* = 7.4 Hz, 3H). ¹³C NMR (100 MHz, Chloroform-*d*) δ 165.96, 164.81, 144.91, 121.47, 120.81, 113.75, 54.51, 51.79, 45.70, 31.42, 28.68, 22.24, 13.93.

2-(2-Hydroxypropyl) 4-methyl 5-methyl-1-propyl-1H-pyrrole-2,4-dicarboxylate (Ppe): ¹H NMR (400 MHz, Chloroform-*d*) δ 7.39 (s, 1H), 4.25 (ddd, *J* = 10.4, 7.9, 4.1 Hz, 3H), 4.15–4.06 (m, 2H), 3.81 (s, 3H), 2.58 (s, 3H), 1.74–1.68 (m, 2H), 1.27 (d, *J* = 6.1 Hz, 3H), 0.94 (t, *J* = 7.4 Hz, 3H). ¹³C NMR (100 MHz, Chloroform-*d*) δ 165.09, 160.66, 141.92, 120.55, 119.94, 112.31, 69.22, 66.27, 51.03, 46.66, 24.05, 19.19, 11.29, 11.03.

The FTIR spectrum of compound 3, Gpe, and Ppe is presented in Figure 3a. In the spectrum, the peaks at 3432 and 3467 cm⁻¹ corresponded to the stretching vibration of the -OH group in the structures of Gpe and Ppe, respectively. The group was a typical functional group in the polyol structure, while the target compounds retained the characteristic absorption peak of compound 3, indicating that Gpe and Ppe were successfully synthesized. As shown in Figure 3b, the calculated values of *m/z* with H added for Gpe and Ppe were 300.1442 and 284.1492, respectively, and those found were 300.1438 and 284.1490. Therefore, combined with Figures 2a,b and 3a,b, it showed that the structures of Gpe and Ppe synthesized were the target compounds, so follow-up performance tests and applications were carried out.

3.2. Evaluation of the Hygroscopicity and Moisturizing Properties of Gpe and Ppe. **3.2.1. Effect of Gpe and Ppe on Moisture Retention and Absorption of the Tobacco Shred.** Additional research on difference in moisture absorption and retention between Gpe and Ppe was performed. The results are shown in Figure 4a,b, respectively. As provided in Figure 4a, the moisture content at RH 32% of the tobacco shred samples decreased with desorption time, and

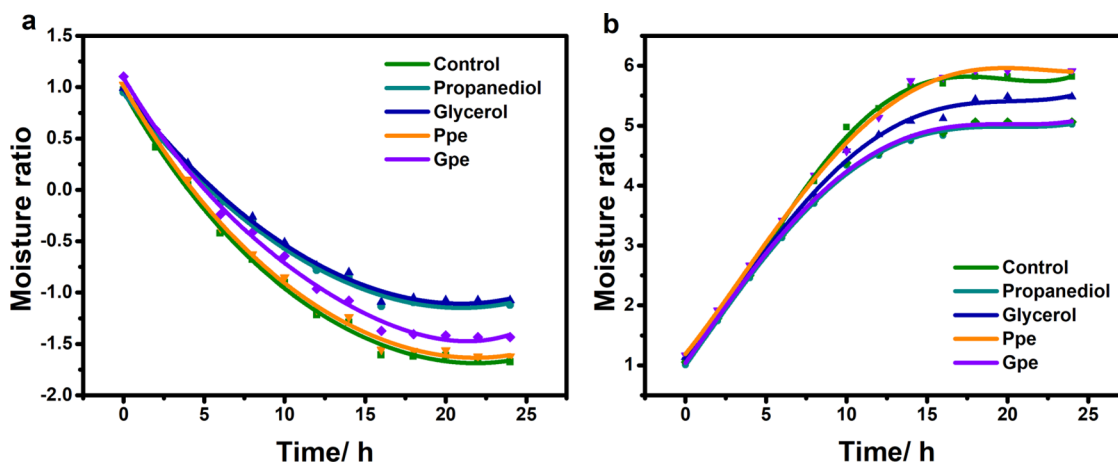


Figure 5. Poly4 model curves of the moisture ratio of tobacco at 22 °C and RH = 32% (a) and RH = 84% (b).

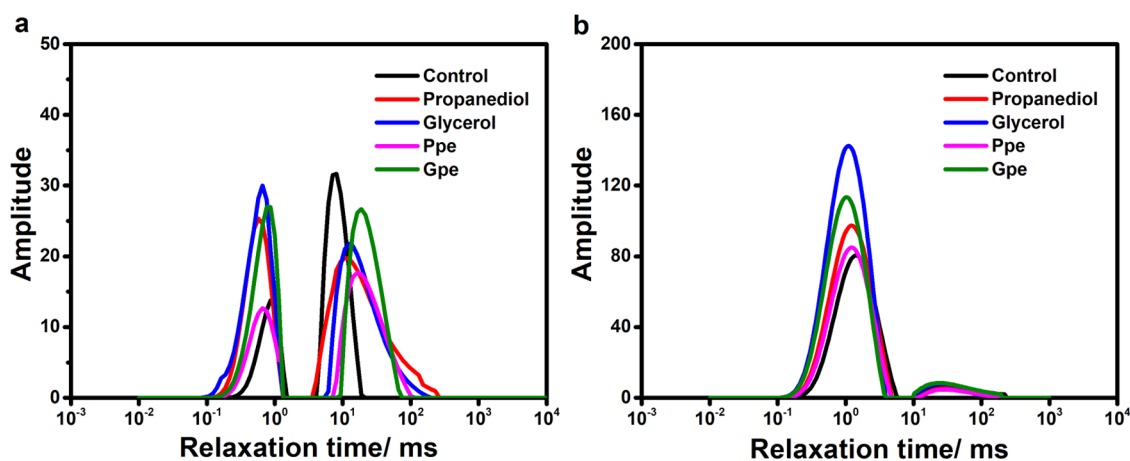


Figure 6. Transverse relaxation time of the tobacco shred at 22 °C and RH = 32% (a) and RH = 84% (b).

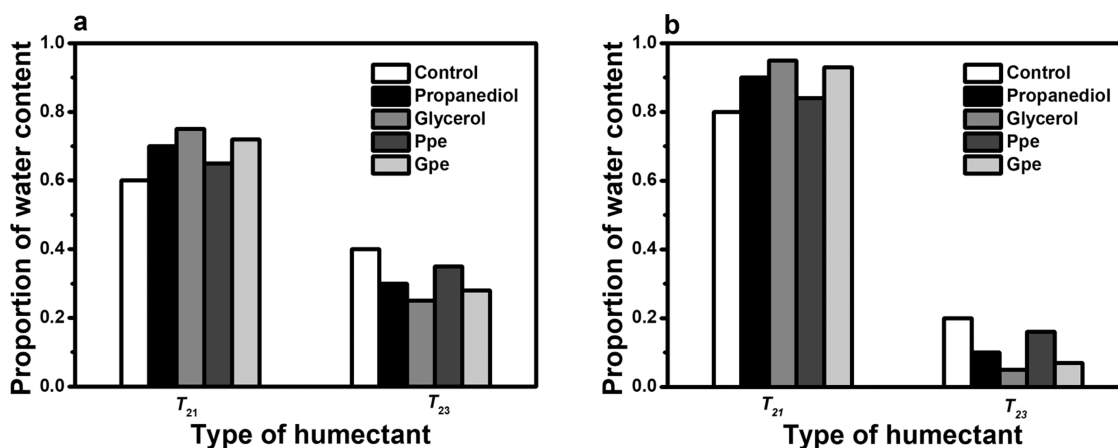


Figure 7. Proportion of the water content of the tobacco shred at 22 °C and RH = 32% (a) and RH = 84% (b).

all samples showed nearly identical drop trends in the first 16 h, and then, they achieved equilibrium at 24 h. The moisture amounts from the control, propanediol, glycerol, Ppe, and Gpe were 3.30, 4.26, 4.40, 3.51, and 4.28%, respectively. As shown in Figure 4b (RH = 84%), the moisture content of the tobacco shred increased with time increasing. After adding five humectants, the moisture contents of the tobacco shred increased quickly for the first 10 h, then slowed down, and stabilized after 24 h. The moisture contents of the control,

propanediol, glycerol, Ppe, and Gpe reached 33.26, 35.10, 37.41, 33.66, and 35.31%, respectively.

As seen in Figure 4a,b, the moisture retention and absorption ability of Gpe was greater than that of the control, while less than that of glycerol. For Ppe, it was greater than that of the control but less than that of propanediol. Over all, the adsorption capacity of the tobacco shred with Gpe and Ppe was restricted. The important reason might be that the number of hydroxyl groups (-OH) played a decisive role. The ability of

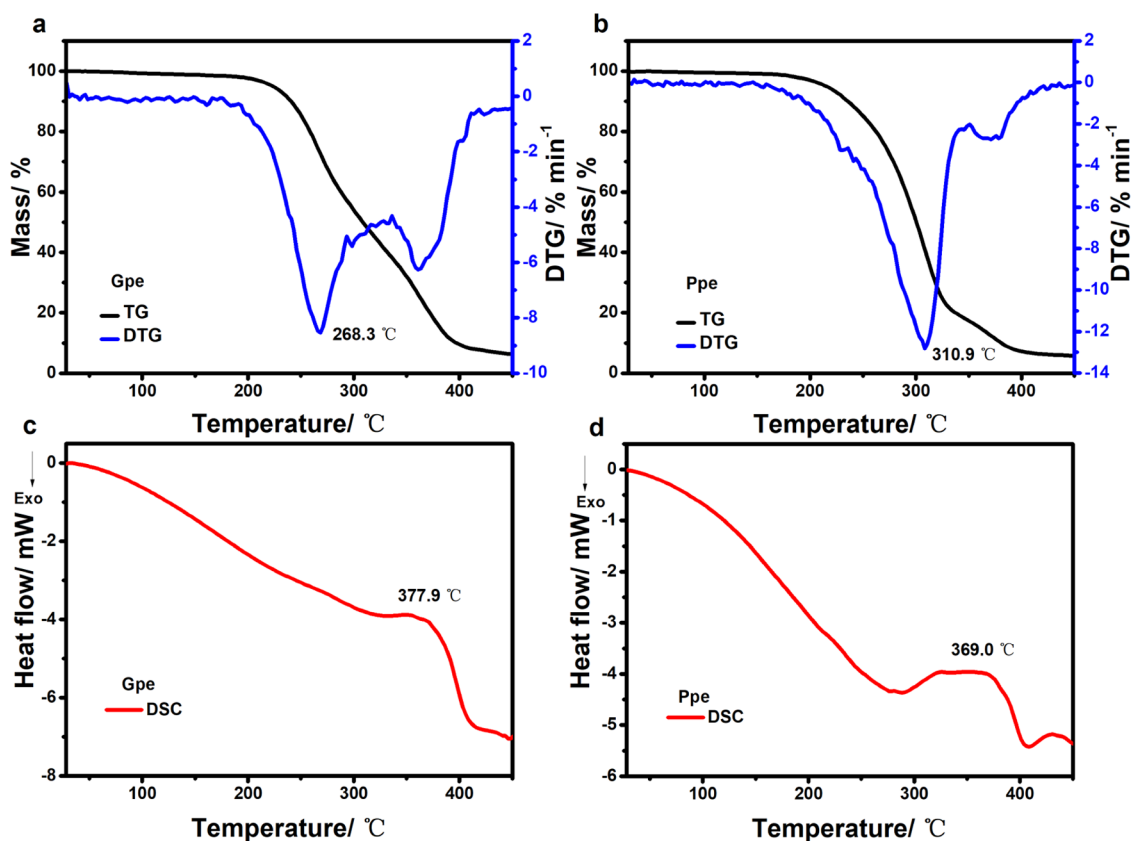


Figure 8. TG-DTG curves of Gpe (a), TG-DTG curves of Ppe (b), DSC curves of Gpe (c), and DSC curves of Ppe (d).

the hydroxyl group to create hydrogen bonds with water molecules enhances the ability to store and absorb water.^{34,35}

3.2.2. Dynamic Model of Moisture Desorption and Absorption. The desorption and adsorption models could be used to describe the relationship between the time and internal moisture ratio of the tobacco shred. Tables 1 and 2 show the fitting of the three models with the corresponding R^2 and MRSE values. Comparing the three models, the Poly4 model displayed the best R^2 and RMSE values. Poly4 was the optimal model for characterizing the moisture change in the tobacco shred with increasing time, while the highest model fitting degree R^2 reached 0.9999 and the RMSE was 0.0001. Therefore, Poly4 could accurately describe and predict the moisture change law (dynamic process) of the tobacco shred before the adsorption or desorption of the cut tobacco reaches equilibrium in different humidity environments.

3.2.3. Optimized Model Fitting Parameters. The values of each group of constants calculated according to the Poly4 model are listed in Tables 3 and 4 in different humidity environments. It was shown that the values of the tobacco shred samples were significantly different because of the characteristics of the humectants. The values reflected the speed of water loss or absorption rate of a certain sample. The Poly4 model curves of the moisture ratio of tobacco are shown in Figure 5a (RH = 32%) and 5b (RH = 84%).

3.2.4. Water Distribution and Migration of the Tobacco Shred with Different Humectants. The capacity to hold and absorb water is improved by the hydroxyl group's capacity to form hydrogen bonds with water molecules. Shorter T_2 values correlated with stronger binding and less water mobility, which showed water distribution and the interaction between water and other macromolecules.^{36,37} The inversion spectral curves

of the tobacco shred are shown in Figure 6a,b. T_{21} and T_{23} , two distinct peaks that represented two water fractions with distinct molecular environments, were studied and determined. The bound water had the smallest relaxation time (T_{21}), and free water exiting in the surface had the longest relaxation time (T_{23}).⁶ It should be noted that strongly bonded states, such as hydroxyl and carboxyl groups, are hydrophilic groups, which are denser and more stable than immobilized water and have relaxation times of less than 1 ms.³⁸ The corresponding relative areas in Figure 6a,b were marked as T_{21} and T_{23} , which were listed as the tobacco shred's proportional contents of bound water and free water, respectively. T_{21} was shorter in the tobacco shred with Gpe and Ppe than that of the control and longer than that of glycerol and propanediol in the different humidity environments (RH = 32 and 84%). In the tobacco shred containing Gpe, Ppe, propanediol, and glycerol, the mobility of the water reduced the water loss that took longer time or required outside effort. The outcomes could be explained by that the four groups could lock water by chemical bonding. Increased hydrogen bonds might develop between the moisturizer's hydroxyl group (-OH) and water molecules, making it harder or more time-consuming to lose water, and strengthen the interaction between the tobacco shred and water molecules. Combined (Figure 6a,b), the water locking effect of Gpe and Ppe was significantly higher than that of the control, while it was slightly lower than that of glycerol and propanediol.

As shown in Figure 7a, the area of the T_{21} band varied in the following order: glycerol > Gpe > propanediol > Ppe > control. In Figure 7b, the order was glycerol > propanediol > Gpe > Ppe > control. At 32% relative humidity and 22 °C, the bound water contents of the tobacco shred-control, tobacco shred-

Table 5. Pyrolysis Products of Gpe

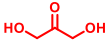


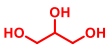
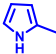
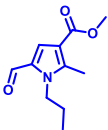
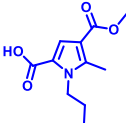
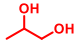
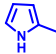
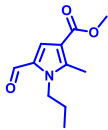
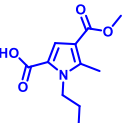
Peak	RT/min	Pyrolysis product	Match/%	Relative content/%	
				350	400
1	3.27	 1,3-Dihydroxypropan-2-one	88	44.92	8.10
2	4.67	 Pentanal	89	-	0.21
3	5.26	 Butanal	90	-	0.13
4	7.31	 Glycerol	88	9.86	14.83
5	24.16	 2-Methyl-1H-pyrrole	85	23.71	73.98
6	28.28	 Methyl 5-formyl-2-methyl-1-propyl-1H-pyrrole-3-carboxylate (compound 2)	85	16.16	2.70
7	34.57	 4-(Methoxycarbonyl)-5-methyl-1-propyl-1H-pyrrole-2-carboxylic acid (compound 3)	84	4.63	-

Table 6. Pyrolysis Products of Ppe

Peak	RT/min	Pyrolysis products	Match/%	Relative content/%	
				350	400
1	4.62	 1,2-Propanediol	90	8.37	41.48
2	23.89	 2-Methyl-1H-pyrrole	86	45.12	37.86
3	28.28	 Methyl 5-formyl-2-methyl-1-propyl-1H-pyrrole-3-carboxylate (compound 2)	87	33.16	14.62
4	34.45	 4-(Methoxycarbonyl)-5-methyl-1-propyl-1H-pyrrole-2-carboxylic acid (compound 3)	85	3.54	-

propanediol, tobacco shred-glycerol, tobacco shred-Ppe, and tobacco shred-Gpe were 60, 70, 75, 65, and 72%, respectively (Figure 7a), while the bound water contents of these groups

were 80, 91, 93, 82, and 90% at RH 84% and 22 °C (Figure 7b). Thus, the content of bound water in the tobacco shred was probably due to the hydrophilic groups (hydroxyl groups)

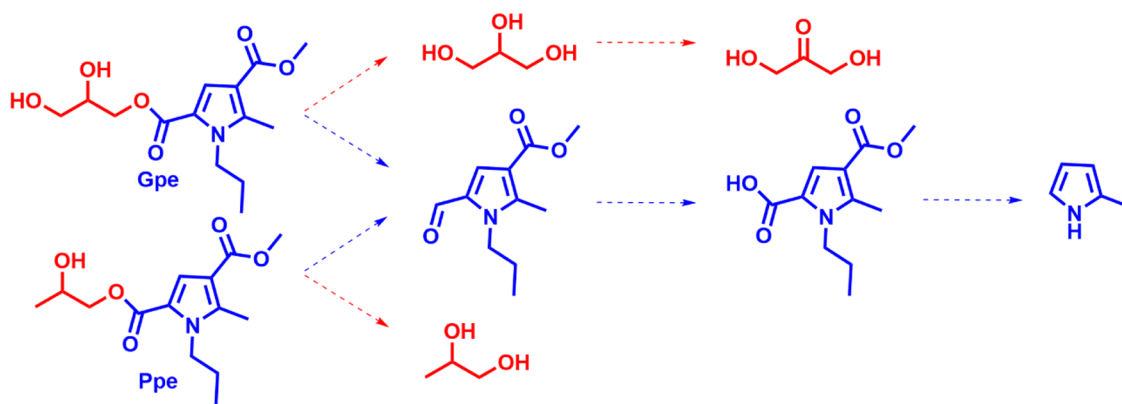


Figure 9. Pyrolysis mechanism of Ppe and Gpe.

derived from glycerol, Gpe, propanediol, and Ppe. The number of hydroxyl groups in glycerol and propanediol was greater than that of Gpe and Ppe, resulting in the highest equilibrium moisture content. These results also supported the findings of earlier experiments that Gpe and Ppe could reduce the strong hygroscopicity of glycerol and propanediol, respectively, and meanwhile maintain a certain moisture absorption and moisturizing capacity compared to the control.

3.3. Thermal Analysis of Gpe and Ppe. **3.3.1. TG-DTG and DSC Analysis of Gpe and Ppe.** Figure 8a,b shows the TG-DTG curves for Gpe and Ppe, respectively. The primary mass change stage of Gpe occurred between 217 and 450 °C, and a peak temperature of 268.3 °C was reached to attain the highest breakdown rate. The highest temperature for Ppe was 310.9 °C, with the main stage being between 203 and 450 °C. The mass loss (TG) of Gpe and Ppe both dropped sharply by 94% as the temperature increased. When the mass change stage was finished, the residue was charred at high temperatures, and only around 6% of its original weight was lost.

The DSC curves of Gpe and Ppe are shown in Figure 8c,d. The enthalpy changes of the synthesized compounds were documented, and the peak temperature of the DSC curves was identified by thermal analysis. It was shown that the endothermic peak temperatures of Gpe and Ppe were 377.9 and 369.0 °C, respectively. At this stage, the small molecules of solid or liquid substances generated by the degradation of the samples might be further decomposed into gaseous substances due to heat absorption. TG-DTG and DSC analyses provided a temperature basis for the analysis of pyrolysis products of the samples, and the quantitative and qualitative analyses of the pyrolysis products of Gpe and Ppe could be implemented in the next experiment.

3.3.2. Pyrolysis Analysis of Gpe and Ppe. In light of the TG-DTG and DSC analysis results, the pyrolysis conditions were designed in an atmosphere of the mixture of 91% nitrogen and 9% oxygen at 350 and 400 °C, and Tables 5 and 6 list the small-molecule pyrolysis products from Gpe and Ppe, respectively.

In Table 5, seven products were observed from the pyrolysis of Gpe at temperatures of 350 and 400 °C *via* GC-MS. Among them, 1,3-dihydroxypropan-2-one (44.92%), glycerol (9.86%), 2-methyl-1H-pyrrole (23.71%), compound 2 (16.16%), and compound 3 (4.63%) were obtained at the temperature of 350 °C, while at the temperature of 400 °C, the pyrolysis products were 1,3-dihydroxypropan-2-one (8.10%), pentanal (0.21%), butanal (0.13%), glycerol (14.83%), 2-methyl-1H-pyrrole

(73.98%), and compound 2 (2.70%), which were recorded *via* GC-MS.

In Table 6, the pyrolysis products from Ppe were 1,2-propanediol (8.37%), 2-methyl-1H-pyrrole (45.12%), compound 2 (33.16%), and compound 3 (3.54%) at the temperature of 350 °C. However, 1,2-propanediol (41.48%), 2-methyl-1H-pyrrole (37.86%), and compound 2 (14.62%) were formed at the pyrolysis temperature of 400 °C.

As seen in Tables 5 and S6, sweet substances were obtained from the pyrolysis of Gpe and Ppe, such as 1,3-dihydroxypropan-2-one, 2-methyl-1H-pyrrole, and 1,2-propanediol, which are widely used in the food spice industry.^{13,39} Glycerol and propanediol were the important parts among all the cleavage products of Gpe and Ppe, respectively. It could be concluded that the raw materials (glycerol and propanediol) were obtained again at high temperature. Interestingly, the relative contents of glycerol and propanediol were higher at 400 °C than those at 350 °C. Py-GC/MS study revealed a correlation between the sample chemical structure and the variety and contents of pyrolysis products. According to the combined TG-DTG-DSC analysis, the ester bond (O=C-O) from the samples may break and generate the synthetic substrates that were then decomposed to form other compounds. Then, the pyrolysis mechanism of Gpe and Ppe was inferred.

3.3.3. Pyrolysis Mechanism of Gpe and Ppe. The pyrolysis products were generated under different pyrolysis conditions. As seen in Tables 5 and 6, the pyrolysis temperatures influenced the relative contents of pyrolysis products. As shown in Figure 9, it was believed that glycerol, 1,2-propanediol, and compound 2 were reproduced, resulting from the breaking of the ester bond O=C-O at the 5-position of pyrrole. With the participation of oxygen in an air atmosphere, 1,3-dihydroxypropan-2-one was observed and compound 3 was derived from compound 2 through an oxidation reaction. In addition, 2-methyl-1H-pyrrole could be obtained from the depropyl reaction at the 1-position and decarbonylative reaction of compound 3.¹⁹ These results were consistent with our original ideas of designing the synthetic route of the target compounds. It proved that polyol pyrrole ester derivatives possess thermal stability and had the effect of slow release of flavor in heat-processed foods.

4. CONCLUSIONS

In conclusion, two novel polyol pyrrole esters 2-(2,3-dihydroxypropyl) 4-methyl 5-methyl-1-propyl-1H-pyrrole-2,4-

dicarboxylate (Gpe) and (2-hydroxypropyl) 4-methyl 5-methyl-1-propyl-1*H*-pyrrole-2,4-dicarboxylate (Ppe) were designed, synthesized, and confirmed by ¹H NMR, ¹³C NMR, IR, and HRMS. Then, the hygroscopicity, moisturizing, and thermal behaviors were studied, and the pyrolysis mechanism was inferred. It could be estimated from adsorption, desorption, and low-field NMR tests that the moisture retention and absorption abilities of Gpe and Ppe were stronger than those of the control but weaker than those of glycerol and 1,2-propanediol, respectively. Gpe and Ppe could slow down the adsorption capacity to a certain extent compared to the polyols (glycerol and propanediol). The endothermic peak temperatures for Gpe and Ppe were 377.9 and 369.0 °C, respectively, and their total mass loss reached 94%, according to the results of TG-DTG-DSC. The ester bond from Gpe and Ppe could be cleaved to form pyrolysis products consisting of the raw materials and the substrates, such as glycerol, 1,2-propanediol, and pyrrole derivatives. Therefore, the target compounds (Gpe and Ppe) could solve the problem of poor taste of cigarettes due to the strong water absorption capacity of conventional polyols (glycerol and propanediol) during processing, storage, and smoking of tobacco; meanwhile, they showed thermal stability and could be flavor precursors, which had the effect of sustained release of flavor under high-temperature combustion. Therefore, the two novel polyol pyrrole esters exert good effects on cigarette moisture and flavor enhancement compared to traditional humectants in the tobacco industry.

■ ASSOCIATED CONTENT

SI Supporting Information

The Supporting Information is available free of charge at <https://pubs.acs.org/doi/10.1021/acsomega.2c06683>.

Copies of ¹H NMR, ¹³C NMR, IR, and HRMS spectra of all compounds and copies of ion chromatograms of the pyrolysis products from Gpe and Ppe at 350 and 400 °C (PDF)

■ AUTHOR INFORMATION

Corresponding Authors

Xiaoming Ji – *Flavors and Fragrance Engineering & Technology Research Center of Henan Province, College of Tobacco Science, Henan Agricultural University, Zhengzhou 450002, China*; orcid.org/0000-0001-6848-2964; Email: xiaomingji@henau.edu.cn

Miao Lai – *Flavors and Fragrance Engineering & Technology Research Center of Henan Province, College of Tobacco Science, Henan Agricultural University, Zhengzhou 450002, China*; Email: laimiao@henau.edu.cn

Authors

Wenpeng Fan – *Flavors and Fragrance Engineering & Technology Research Center of Henan Province, College of Tobacco Science, Henan Agricultural University, Zhengzhou 450002, China*

Haiying Tian – *Technology Center, China Tobacco Henan Industrial Co., Ltd., Zhengzhou 450000, China*

Hongli Chen – *Flavors and Fragrance Engineering & Technology Research Center of Henan Province, College of Tobacco Science, Henan Agricultural University, Zhengzhou 450002, China*

Wenjuan Chu – *Technology Center, China Tobacco Henan Industrial Co., Ltd., Zhengzhou 450000, China*

Lu Han – *Technology Center, China Tobacco Henan Industrial Co., Ltd., Zhengzhou 450000, China*

Pengyu Li – *Flavors and Fragrance Engineering & Technology Research Center of Henan Province, College of Tobacco Science, Henan Agricultural University, Zhengzhou 450002, China*

Ziting Gao – *Flavors and Fragrance Engineering & Technology Research Center of Henan Province, College of Tobacco Science, Henan Agricultural University, Zhengzhou 450002, China*

Complete contact information is available at:

<https://pubs.acs.org/10.1021/acsomega.2c06683>

Author Contributions

[§]H.T. and H.C. contributed equally to this study and share the first authorship. W.F.: first draft, revision, editing, conceptualization, and methodology in writing. H.T.: writing the first draft, revision, and editing. H.C.: data curation and investigation. W.C.: data curation and investigation. L.H.: methodology and investigation. P.L.: methodology and investigation. Z.G.: formal analysis and investigation. X.J.: review and editing and supervision. M.L.: review and editing and investigation.

Notes

The authors declare no competing financial interest.

■ ACKNOWLEDGMENTS

This work was supported by China Tobacco Henan Industrial Co., Ltd. (2021410001300098), the Science and Technology Department of Henan Province (152102210058), and Henan Agricultural University (30500845).

■ REFERENCES

- (1) Zhang, X.; Gao, H.; Zhang, L.; Liu, D.; Ye, X. Extraction of essential oil from discarded tobacco leaves by solvent extraction and steam distillation, and identification of its chemical composition. *Ind. Crops Prod.* **2012**, *39*, 162–169.
- (2) Huang, Y.; Du, G.; Ma, Y.; Zhou, J. Predicting heavy metals in dark sun-cured tobacco by near-infrared spectroscopy modeling based on the optimized variable selections. *Ind. Crops Prod.* **2021**, *172*, No. 114003.
- (3) Samejima, T.; Soh, Y.; Yano, T. Moisture sorption isotherms of various tobaccos. *Agric. Biol. Chem.* **1978**, *42*, 2285–2290.
- (4) Samejima, T.; Yano, T. Moisture Diffusion within Shredded Tobacco Leaves. *Agric. Biol. Chem.* **1985**, *49*, 1809–1812.
- (5) Yan, H.; Cai, B.; Cheng, Y.; Guo, G.; Li, D.; Yao, X.; Ni, X.; Phillips, G. O.; Fang, Y.; Jiang, F. Mechanism of lowering water activity of konjac glucomannan and its derivatives. *Food Hydrocolloid.* **2012**, *26*, 383–388.
- (6) Lin, C.; Cui, H.; Wang, X.; Wang, H.; Xia, S.; Hayat, K.; Hussain, S.; Tahir, M. U.; Zhang, X. Regulating water binding capacity and improving porous carbohydrate matrix's humectant and moisture proof functions by mixture of sucrose ester and Polygonatum sibiricum polysaccharide. *Int. J. Biol. Macromol.* **2020**, *147*, 667–674.
- (7) Chou, C.-H.; Sung, T.; Hu, Y.; Lu, H.; Yang, L.; Cheng, K.; Lai, P.; Hsieh, C. Chemical analysis, moisture-preserving, and antioxidant activities of polysaccharides from *Pholiota nameko* by fractional precipitation. *Int. J. Biol. Macromol.* **2019**, *131*, 1021–1031.
- (8) Chi, Y.; Ye, H.; Li, H.; Li, Y.; Guan, Y.; Mou, H.; Wang, P. Structure and molecular morphology of a novel moisturizing exopolysaccharide produced by *Phyllobacterium sp.* 921F. *Int. J. Biol. Macromol.* **2019**, *135*, 998–1005.

- (9) Heck, J. D.; Gaworski, C. L.; Rajendran, N.; Morrissey, R. L. Toxicologic evaluation of humectants added to cigarette tobacco: 13-week smoke inhalation study of glycerin and propylene glycol in fischer 344 rats. *Inhal. Toxicol.* **2002**, *14*, 1135–1152.
- (10) Rainey, C. L.; Shifflett, J. R.; Goodpaster, J. V.; Bezabeh, D. Z. Quantitative analysis of humectants in tobacco products using gas chromatography (GC) with simultaneous mass spectrometry (MSD) and flame ionization detection (FID). *Contrib. Tobacco Res.* **2013**, *25*, 576–585.
- (11) Zhou, C. F.; Qian, P.; Meng, J.; Gao, S. M.; Lu, R. R. Effect of glycerol and sorbitol on the properties of dough and white bread. *Cereal Chem.* **2016**, *93*, 196–200.
- (12) Wang, L.; Cardenas, R. B.; Watson, C. An isotope dilution ultra high performance liquid chromatography-tandem mass spectrometry method for the simultaneous determination of sugars and humectants in tobacco products. *J. Chromatogr. A.* **2017**, *1514*, 95–102.
- (13) Maga, J. A. Pyrroles in foods. *J. Agric. Food Chem.* **1981**, *29*, 691–694.
- (14) Pacyński, M.; Wojtasiak, R. Z.; Szkudlarz, S. M. Improving the aroma of gluten-free bread. *Lwt-Food. Sci. Technol.* **2015**, *63*, 706–713.
- (15) MacLeod, G.; Coppock, B. M. A comparison of the chemical composition of boiled and roasted aromas of heated beef. *J. Agric. Food Chem.* **1977**, *25*, 113–117.
- (16) Mestdagh, F.; Davidek, T.; Chaumonteuil, M.; Folmer, B.; Blank, I. The kinetics of coffee aroma extraction. *Food Res. Int.* **2014**, *63*, 271–274.
- (17) Alasalvar, C.; Shahidi, F.; Cadwallader, K. R. Comparison of natural and roasted Turkish tumbul hazelnut (*Corylus avellana* L.) volatiles and flavor by DHA/GC/MS and descriptive sensory analysis. *J. Agr. Food Chem.* **2003**, *51*, 5067–5072.
- (18) Ai, L.; Liu, M.; Ji, X.; Lai, M.; Zhao, M.; Ren, T. Thermal behavior analysis of two synthesized flavor precursors of N-alkylpyrrole derivatives. *J. Heterocycl. Chem.* **2019**, *56*, 2389–2397.
- (19) Fan, W.; Chu, W.; Tian, H.; Zhang, Z.; Feng, Y.; Gao, Z.; Cheng, B.; Ji, X.; Lai, M. Synthesis and pyrolysis of two novel pyrrole ester flavor precursors. *J. Heterocycl. Chem.* **2022**, *59*, 1397–1406.
- (20) Lee, K. G.; Shibamoto, T. Toxicology and antioxidant activities of non-enzymatic browning reaction products. *Food Rev. Int.* **2002**, *18*, 151–175.
- (21) Ates, E. G.; Domenici, V.; Wojciechowska, M. F.; Gradišek, A.; Kruk, D.; Strmečki, N. M.; Oztop, M.; Ozvural, E. B.; Rollet, A. L. Field-dependent NMR relaxometry for Food Science: Applications and perspectives. *Trends Food Sci. Tech.* **2021**, *110*, 513–524.
- (22) Zhang, L.; McCarthy, M. J. Black heart characterization and detection in pomegranate using NMR relaxometry and MR imaging. *Postharvest Biol. Technol.* **2012**, *67*, 96–101.
- (23) Defraeye, T.; Lehmann, V.; Gross, D.; Holat, C.; Herremans, E.; Verboven, P.; Verlinden, B. E.; Nicolai, B. M. Application of MRI for tissue characterisation of 'Braeburn' apple. *Postharvest Biol. Technol.* **2013**, *75*, 96–105.
- (24) Raffo, A.; Gianferri, R.; Barbieri, R.; Brosio, E. Ripening of banana fruit monitored by water relaxation and diffusion ¹H-NMR measurements. *Food Chem.* **2005**, *89*, 149–158.
- (25) Takeuchi, S.; Maeda, M.; Gomi, Y.; Fukuoka, M.; Watanabe, H. The change of moisture distribution in a rice grain during boiling as observed by NMR imaging. *J. Food Eng.* **1997**, *33*, 281–297.
- (26) Li, J.; Kang, J.; Wang, L.; Li, Z.; Wang, R.; Chen, Z.; Hou, G. G. Effect of water migration between arabinoxylans and gluten on baking quality of whole wheat bread detected by magnetic resonance imaging (MRI). *J. Agri. Food Chem.* **2012**, *60*, 6507–6514.
- (27) Hansen, C. L.; Thybo, A. K.; Bertram, H. C.; Viereck, N.; Berg, F.; Engelsens, S. B. Determination of dry matter content in potato tubers by low-field nuclear magnetic resonance (LF-NMR). *J. Agri. Food Chem.* **2010**, *58*, 10300–10304.
- (28) Milczarek, R. R.; Saltveit, M. E.; Garvey, T. C.; McCarthy, M. J. Assessment of tomato pericarp mechanical damage using multivariate analysis of magnetic resonance images. *Postharvest Biol. Technol.* **2009**, *52*, 189–195.
- (29) Straadt, I. K.; Thybo, A. K.; Bertram, H. C. NaCl-induced changes in structure and water mobility in potato tissue as determined by CLSM and LF-NMR. *Lwt-Food. Sci. Technol.* **2008**, *41*, 1493–1500.
- (30) Scholze, B.; Hanser, C.; Meier, D. Fraction from fast pyrolysis liquids (pyrolytic lignin): Part II. GPC, carbonyl groups, and ¹³C-NMR. *J. Anal. Appl. Pyrol.* **2001**, *58*, 387–400.
- (31) Gerber, L.; Eliasson, M.; Trygg, J.; Moritz, T.; Sundberg, B. Multivariate curve resolution provides a high-throughput data processing pipeline for pyrolysis-gas chromatography/mass spectrometry. *J. Anal. Appl. Pyrol.* **2012**, *95*, 95–100.
- (32) Li, R.; Yin, X.; Zhang, S.; Yang, J.; Zhao, M. Preparation and pyrolysis of two Amadori analogues as flavor precursors. *J. Anal. Appl. Pyrolysis* **2021**, *160*, 105357–105367.
- (33) Li, H. F.; Xu, J.; Liu, Y. M.; Ai, S. B.; Qin, F.; Li, Z. W.; Zhang, H. R.; Huang, Z. Antioxidant and moisture-retention activities of the polysaccharide from *Nostoc commune*. *Carbohydr. Polym.* **2011**, *83*, 1821–1827.
- (34) Qin, C.; Du, Y.; Xiao, L.; Liu, Y.; Yu, H. Moisture retention and antibacterial activity of modified chitosan by hydrogen peroxide. *J. Appl. Polym. Sci.* **2002**, *86*, 1724–1730.
- (35) Wang, J.; Jin, W.; Hou, Y.; Niu, X.; Zhang, H.; Zhang, Q. Chemical composition and moisture-absorption/retention ability of polysaccharides extracted from five algae. *Int. J. Biol. Macromol.* **2013**, *57*, 26–29.
- (36) Wei, S.; Tian, B. Q.; Jia, H. F.; Zhang, H. Y.; He, F.; Song, Z. P. Investigation on water distribution and state in tobacco leaves with stalks during curing by LF-NMR and MRI. *Dry Technol.* **2018**, *36*, 1515–1522.
- (37) Xu, F.; Jin, X.; Zhang, L.; Chen, X. D. Investigation on water status and distribution in broccoli and the effects of drying on water status using NMR and MRI methods. *Food Res. Int.* **2017**, *96*, 191–197.
- (38) Lin, S.; Yang, S.; Li, X.; Chen, F.; Zhang, M. Dynamics of water mobility and distribution in soybean antioxidant peptide powders monitored by LF-NMR. *Food Chem.* **2016**, *199*, 280–286.
- (39) Shipar, M. A. H. Formation of the Heyns rearrangement products in dihydroxyacetone and glycine Maillard reaction: A computational study. *Food Chem.* **2006**, *97*, 231–243.
- (40) Wang, H.; Cui, H.; Wang, X.; Lin, C.; Xia, S.; Hayat, K.; Hussain, S.; Tahir, M. U.; Zhang, X. Metal complexed-enzymatic hydrolyzed chitosan improves moisture retention of fiber papers by migrating immobilized water to bound state. *Carbohydr. Polym.* **2020**, *235*, No. 115967.